Direct calculation of optical absorption amplitudes for trivalent rare-earth ions in $LiYF_4$

Daniel Åberg[1] and Sverker Edvardsson[2]
[1]*Condensed Matter Theory Group, Uppsala University, Box 530, S-751 21 Uppsala, Sweden*
[2]*Department of Physics, Mid Sweden University, S-851 70 Sundsvall, Sweden*
(Received 8 September 2000; revised manuscript received 5 October 2001; published 7 January 2002)

The approximations within the Judd-Ofelt theory are eliminated by an explicit reformulation of the absorption amplitude for $f\leftrightarrow f$ dipole transitions in terms of determinantal product states and perturbed functions. By considering the crystal-field and spin-orbit perturbations we obtain expressions for amplitudes of the type $\langle\phi^1_{cf}|d^1_q|\phi^0\rangle$, $\langle\phi^1_{cf}|d^1_q|\phi^1_{so}\rangle$, and $\langle\phi^1_{cf}|d^1_q|\phi^1_{cf}\rangle$. The latter two are third-order results, going beyond the standard Judd-Ofelt theory. There are no experimentally fitted parameters used in the amplitude calculations. Crystal-field parameters A_{tp} needed for the intensity calculations are calculated using the self-consistent electrostatic model. Polarized absorption spectra are calculated for Nd^{3+}, Ho^{3+}, Er^{3+}, or Tm^{3+} in $LiYF_4$. Very good agreement with experiment is, in general, observed. The contribution from the third-order terms $\langle\phi^1_{cf}|d^1_q|\phi^1_{so}\rangle$ and $\langle\phi^1_{cf}|d^1_q|\phi^1_{cf}\rangle$ are seen to be small in comparison with $\langle\phi^1_{cf}|d^1_q|\phi^0\rangle$.

DOI: 10.1103/PhysRevB.65.045111 PACS number(s): 78.20.Bh, 32.70.Cs, 78.40.−q

I. INTRODUCTION

In the present work we derive explicit theoretical expressions for transition amplitudes between states within the f shell in order to make numerical computations from first principles possible. One advantage of deriving a more accurate model is that discrepancies between experiment and calculations will almost certainly only be due to estimation problems of the crystal field parameters A_{tp} or in special cases [light rare earths] possibly correlation. We start with the oscillator-strength expression (1) in the classic article by Judd;[1] and instead of using perturbation theory with problematic excited states, we immediately apply the perturbed-functions approach, see, e.g., Ref. 2 for an original reference. For $f\leftrightarrow f$ transitions, the most important modifications to the free-ion wave functions are assumed to arise from crystal field, spin orbit, and correlation interactions. Here, we consider perturbed functions resulting from the crystal field and spin-orbit interactions. These give rise to transition amplitude elements of the type: $\langle\phi^1_{cf}|d^1_q|\phi^0\rangle$, $\langle\phi^1_{cf}|d^1_q|\phi^1_{so}\rangle$, and $\langle\phi^1_{cf}|d^1_q|\phi^1_{cf}\rangle$. This is interesting since it has been speculated earlier in the literature that third-order effects such as $\langle\phi^1_{cf}|d^1_q|\phi^1_{so}\rangle$ and $\langle\phi^1_{cf}|d^1_q|\phi^1_{cf}\rangle$ might be important.[3–5] Smentek and co-workers showed that also correlation effects on transition intensities can be significant.[6,7] Also for light atoms, correlation usually plays an important role in atomic transitions.[8] The quantitative importance of these effects on $f\leftrightarrow f$ transitions will be presented in a separate communication shortly.

The perturbed-functions approach is an elegant way to solve the perturbation problem since expansion of the wave function in terms of excited states and excited energies is completely avoided. This method is applied here and avoids or goes beyond the following approximations within the Judd-Ofelt theory (J-O).[1,9]

(1) J-O only includes second-order terms, perturbed by the crystal field, while here we treat both crystal-field and spin-orbit interactions up to third order.

(2) The perturbing configurations are limited to only $4f^{N-1}5d$ and $4f^{N-1}n'g$ using an approximate closure treatment, while here the analog would be that we modify each $4f$ orbital according to

$$|4f\rangle\rightarrow|4f\rangle+\sum_{n'}^{\infty}\sum_{l'=0}^{10}c_{n'l'}|n'l'\rangle$$

including the continuum states (the quantum numbers m_l and m_s are omitted for clarity). The sum over $n'l'$ is restricted to unoccupied orbitals. Note that the above expression never appears explicitly in the perturbed-functions approach.

(3) The J-O theory uses a single value for the energy of each perturbing configuration in order to allow closure to be done. The energy denominator is also the same for all states in the initial $4f^N$ configuration, thus simplifying the problem making the energy denominators independent of the real initial and final states. This also implies that the $nl^{N-1}n'l'$ configuration lies far above the nl^N configuration. These approximations are completely avoided in the present work, since the wave functions in the perturbed functions approach are not expanded in terms of excited configuration wave functions and energies; see Judd's Eq. (4).[1]

(4) Intermediate coupling is assumed in the J-O theory implying that J is a good quantum number. This is unfortunately not true for crystal-field states (J-J mixing). The present work does not suffer from this, since no particular coupling is enforced, i.e., fully mixed eigenvectors are used in present intensity theory.

(5) The original J-O theory assumes that the crystal-field levels of the ground state are equally populated. Boltzmann-distributed populations are used here as well as in other variants of the J-O theory, see, e.g., Ref. 10.

Applying the perturbed-functions approach together with fully mixed Stark eigenfunctions (from the energy matrix, see Ref. 11) we avoid the intrinsic approximations of the Judd-Ofelt theory.

In the present work we choose to study the host material RE:$LiYF_4$ (YLF) with RE=Nd^{3+}, Ho^{3+}, Er^{3+}, or Tm^{3+}, since YLF is well covered in a great number of

publications.[12–23] The crystal field parameters are approximated using the electrostatic self-consistent field approach.[23,24] For ionic solids this model seems to be sufficient, see, e.g., Refs. 12, 13, and 25. The resulting theoretical spectra are actually quite promising, maybe particularly so for Ho:YLF, where the correlation contributions to intensities are expected to be small. Correlation influences are known to be much more important for loosely bound electrons (e.g., for ions in the beginning of the lanthanide series such as Nd).

Except for the basic research interest, another good reason to investigate the predictability of theory is the possibility to develop more refined models to optimize certain optical properties in rare-earth doped optical materials.

II. THEORETICAL BACKGROUND

The spectra of $f \leftrightarrow f$ transitions of a rare-earth ion are determined by its wave functions and the corresponding energies. These are defined by the Schrödinger equation $\hat{H}\Psi_k = E_k\Psi_k$ with the usual Hamiltonian $\hat{H} = \hat{H}_0 + \hat{H}'$, where

$$\hat{H}' = \sum_{i<j} \frac{1}{r_{ij}} + \sum_i \xi(r_i)\hat{l}_i \cdot \hat{s}_i + \sum_i \sum_{tp} B_{tp} C_{tp}(\theta_i, \phi_i) + \frac{1}{2}\vec{B} \cdot \sum_i (\hat{l}_i + 2\hat{s}_i),$$

given in atomic units. The C_{tp} operators are renormalized spherical harmonics; that is, $C_{tp} = \sqrt{(4\pi/(2t+1)}Y_{tp}$, and a crystal field parameter B_{tp} (Wybourne notation) is related to A_{tp} (see Sec. IV) through $B_{tp} = (1-\sigma_t)\langle r^t \rangle_{nl} A_{tp}$ for even t only.[2] Numerical values of the shielding factor σ_t and $\langle r^t \rangle_{nl}$ can be found in Ref. 12. The last term in $\hat{H}'$ takes into account the Zeeman splittings and changes in the eigenvectors due to an external magnetic field. The unperturbed Schrödinger equation $\hat{H}_0\Psi_k^0 = E_k^0\Psi_k^0$ is solved using the relativistic Hartree-Fock method of Cowan.[26] In energy calculations the perturbed Hamiltonian is usually replaced by

$$\hat{H}'_{eff} = \sum_{k=2,4,6} F^k(4f,4f)\hat{f}_k + \sum_i \xi(r_i)\hat{l}_i \cdot \hat{s}_i + \alpha\hat{L}^2 + \beta\hat{G}(G_2) + \gamma\hat{G}(R_7) + \sum_{i=2,3,4,6,7,8} T^i\hat{t}_i + \sum_i \sum_{tp} B_{tp} C_{tp}(\theta_i, \phi_i) + \frac{1}{2}\vec{B} \cdot \sum_i (\hat{l}_i + 2\hat{s}_i). \quad (1)$$

Here F^k are the Slater integrals and $\hat{f}_k = \hat{C}^k(1) \cdot \hat{C}^k(2)$ are angular parts of the electrostatic interaction. $\alpha\hat{L}^2$, $\beta\hat{G}(G_2)$, and $\gamma\hat{G}(R_7)$ are the configuration-interaction (CI) operators of Rajnak and Wybourne,[27] and the $\hat{t}_i$ are the three-particle CI operators of Judd.[28] This effective Hamiltonian only employs even crystal-field parameters and operates completely within the f space. The correlation crystal-field contribution to the energy splitting is neglected since its contribution to the energy is small and the fitted one-electron B_{tp}'s include many of its effects.[29] The free-ion parameters used in present work are from Ref. 30. The even B_{tp} parameters are listed in Table I. The reason for using fitted B_{tp} parameters for the energy matrix is to obtain the best possible eigenvectors as starting wave functions. However, note that all $f \leftrightarrow f$ dipole transitions are still forbidden at this level. After a diagonalization, the correct zeroth-order states are usually described by

TABLE I. B_{tp} parameters in cm^{-1} for triply ionized rare earths in $LiYF_4$ (Wybourne normalization).

	Nd[a]	Ho[b]	Er[c]	Tm[d]
B_{20}	441	410	314	333
B_{40}	−906	−615	−625	−648
B_{44}	1115	819	982	876
B_{60}	−26.3	−27.9	−32.4	−141
Re B_{64}	1073	677	584	623
Im B_{64}	20.6	32.8	171	3

[a]Reference 49.
[b]Reference 50.
[c]Reference 51.
[d]Reference 41.

$$\chi_i^0 = \sum_{LSJMWU} c^i_{LSJMWU} |nfLSJMWU\rangle,$$

where WU is shorthand for $(w_1w_2w_3)(u_1u_2)$ and these are additional quantum numbers to distinguish states with the same $SLJM$, see Ref. 31. Another equivalent representation is of course the Slater-determinant basis, which then instead gives eigenfunctions of the following form (program available in Ref. 11):

$$\chi_i^0 = \sum_a c_a^i \{\phi_1^0\phi_2^0 \ldots \phi_N^0\}_a .$$

The use of determinantal product states is clearly a disadvantage for the group theoretical aspects of the states, but is indeed appealing with regard to the simplicity in calculating matrix elements and amplitudes for any number of electrons. We also want to use a simple, but general, representation so that the derivations of the various transition amplitudes within the perturbed-functions approach become as straightforward as possible.

The oscillator strength P_q for an electric-dipole transition of polarization q between $\Psi_i \rightarrow \Psi_f$ is given by[1]

$$P_q = \chi[8\pi^2 m\nu/h]|\langle\Psi_i|D_q^1|\Psi_f\rangle|^2 \frac{e^{-E_i/kT}}{\sum_j e^{-E_j/kT}}. \quad (2)$$

Here $D_q^1 = \Sigma_j d_q^1(j) = \Sigma_j r_j C_{1q}(\theta_j, \phi_j)$ and χ is the Lorentz local-field correction. The last factor makes sure that occupations of the ground states are Boltzmann distributed. Here the Stark levels will be populated for room temperature. In the case of degenerate Stark levels (odd number of electrons) or in the case of accidental degeneracy, the squared transition amplitude of Eq. (2) is replaced by

$$\frac{1}{\deg(i)} \sum_{k=1}^{\deg(i)} \sum_{l=1}^{\deg(f)} |\langle \Psi_{ik}|D_q^1|\Psi_{fl}\rangle|^2,$$

where the indices k and l represent the substates of the degenerate levels. Since the eigenfunctions of the energy matrix belong to f space and D_q^1 is an odd operator, the transition amplitudes $\langle \chi_i^0|D_q^1|\chi_f^0\rangle$ are identically equal to zero.

The appropriate start for calculating the dipole-transition amplitudes using Slater determinants is given by

$$\langle \Psi_i|D_q^1|\Psi_f\rangle = \sum_{ab} c_a^{i*} c_b^f \langle \{\phi_1 \cdots \phi_N\}_a|D_q^1|\{\phi_1 \cdots \phi_N\}_b\rangle, \tag{3}$$

where each spin orbital $\phi_k = \phi_k^0 + \phi_k^1 + \cdots$.

As long as each spin orbital ϕ_k satisfies the orthonormality condition

$$\langle \phi_m|\phi_n\rangle = \delta_{mn}, \tag{4}$$

the standard rules for matrix elements of Slater determinants are valid. Equation (3) then reduces to a sum of one-electron dipole transition amplitudes of the type $\langle \phi_m|d_q^1|\phi_n\rangle$.

III. THE PERTURBED-FUNCTIONS APPROACH

Our purpose here is to mix in perturbed wave functions in order to obtain nonvanishing transition amplitudes. As is well known, for one-particle perturbing operators, the Schrödinger equation $(\hat{H}_0 + \hat{H}')\Psi_k = E_k\Psi_k$ can be separated into one-particle equations

$$(\hat{h}_0 + \hat{h}')\phi_k = \varepsilon_k \phi_k, \tag{5}$$

where $\hat{h}_0 = -\frac{1}{2}\nabla^2 + \hat{v}_{HF}$. In general, the exact solutions ϕ_k of Eq. (5) cannot be determined. Instead, these are expanded here by $\phi_k \approx \phi_k^0 + \phi_k^1$ and then inserted into the determinants. The approximate wave functions are then given by:

$$\Psi \approx \sum_a c_a \{(\phi_1^0 + \phi_1^1) \cdots (\phi_N^0 + \phi_N^1)\}_a. \tag{6}$$

The zeroth-order spin orbitals ϕ_k^0, energies ε_k^0, and effective potentials are computed using the program by Cowan,[26] where both relativistic and nonrelativistic Hartree-Fock calculations are possible. The aim is now to find the perturbed functions ϕ_k^1, not forgetting to satisfy the orthogonality condition, i.e., Eq. (4). We then wish to compute the dipole-transition amplitude of Eq. (3), but instead using the approximate wave functions of Eq. (6).

The one-particle perturbations considered here are the crystal-field and spin-orbit operators,

$$\hat{h}' = \hat{h}_{cf} + \hat{h}_{so} = \sum_{tp} A_{tp} r^t C_{tp} + \xi_{nl}(r)\hat{l}\cdot\hat{s}.$$

The spin-orbit function is approximated by

$$\xi_{nl}(r) = \frac{\alpha^2}{2}\frac{1}{r}\frac{dv_{HF}(nl)}{dr}.$$

From the first-order degenerate perturbation equation it is seen that the one-electron function ϕ_k^1 can be divided into a crystal-field and a spin-orbit function; $\phi_k^1 = \phi_{k,cf}^1 + \phi_{k,so}^1$. The transition amplitude $\langle \phi_m|d_q^1|\phi_n\rangle$ can then be written as

$$\langle \phi_m|d_q^1|\phi_n\rangle \approx \langle \phi_m^0 + \phi_{m,cf}^1 + \phi_{m,so}^1|d_q^1|\phi_n^0 + \phi_{n,cf}^1 + \phi_{n,so}^1\rangle. \tag{7}$$

The term $\langle \phi_m^0|d_q^1|\phi_n^0\rangle$ vanishes because of parity and so do $\langle \phi_{m,so}^1|d_q^1|\phi_n^0\rangle$, $\langle \phi_m^1|d_q^1|\phi_{n,so}^0\rangle$, and $\langle \phi_{m,so}^1|d_q^1|\phi_{n,so}^1\rangle$. The latter three because the spin-orbit operator is a scalar operator, and therefore the angular momenta of the unperturbed and the perturbed wave functions are the same.

We are thus left with the pure crystal-field elements

$$d_{cf\text{-}0} = \langle \phi_{m,cf}^1|d_q^1|\phi_n^0\rangle + \langle \phi_m^0|d_q^1|\phi_{n,cf}^1\rangle, \tag{8}$$

$$d_{cf\text{-}cf} = \langle \phi_{m,cf}^1|d_q^1|\phi_{n,cf}^1\rangle \tag{9}$$

and the mixed crystal-field spin-orbit contribution

$$d_{cf\text{-}so} = \langle \phi_{m,cf}^1|d_q^1|\phi_{n,so}^1\rangle + \langle \phi_{m,so}^1|d_q^1|\phi_{n,cf}^1\rangle. \tag{10}$$

A. Pure crystal-field contribution

In order to derive explicit expressions for Eq. (8) we start from the single-particle first-order degenerate perturbation equation

$$(\hat{h}_0 - \varepsilon_{nl})\psi_i^1 = (\varepsilon_i' - \hat{h}_{cf})\Xi_i^0, \tag{11}$$

where Ξ_i^0 denotes a correct zeroth-order function,

$$\Xi_i^0 = \sum_{m_{lk}m_{sk}} d^i_{m_{lk}m_{sk}} \phi_k^0.$$

The $d^i_{m_l m_s}$'s are the coefficients of the ith eigenvector of the matrix h_{cf}, using the $\{\phi_k^0\}$ basis, and the first-order function ψ_i^1 is expanded in the perturbed orbitals according to

$$\psi_i^1 = \sum_{m_{lk}m_{sk}} d^i_{m_{lk}m_{sk}} \phi_{k,cf}^1,$$

where

$$\phi_{k,cf}^1 = \frac{1}{r}\sum_{l'm_l'm_s'} u_{cf}(nlm_{lk}m_{sk} \rightarrow l'm_l'm_s') Y_{l'm_l'}\chi_{m_s'}.$$

The expansions of Ξ_i^0 and ψ_i^1 are then inserted into Eq. (11), and upon multiplying with $Y_{lm_l}\chi_{m_s}$ and integrating over angular and spin coordinates, the left-hand side of Eq. (11) becomes

$$\sum_{m_{lk}m_{sk}} (\hat{h}_0^{l'} - \varepsilon_{nl}) d^i_{m_{lk}m_{sk}} \frac{1}{r} u_{cf}(nlm_{lk} \rightarrow l'm_l'), \tag{12}$$

where

$$\hat{h}_0^{l'} = -\frac{1}{2}\frac{d^2}{dr^2} + \frac{l'(l'+1)}{2r^2} + v_{HF}(nl).$$

The right-hand side now reads

$$\left(\varepsilon_i' d^i_{m_l' m_s'} \delta(l',l) - \sum_{m_{lk} m_{sk}} d^i_{m_{lk} m_{sk}} \sum_{tp} A_{tp} r^t \times \langle l' m_l' | C_{tp} | l m_{lk} \rangle \right) \frac{1}{r} P_{nl}. \quad (13)$$

It is also clear from the matrix equation $h_{cf}\Xi_i^0 = \varepsilon_i' \Xi_i^0$ that

$$\varepsilon_i' d^i_{m_l' m_s'} = \sum_{m_{lk} m_{sk}} d^i_{m_{lk} m_{sk}} \sum_{tp} A_{tp} \langle l' m_l' | C_{tp} | l m_{lk} \rangle \langle r^t \rangle,$$

so the expression (13) now becomes

$$\sum_{m_{lk} m_{sk}} d^i_{m_{lk} m_{sk}} \sum_{tp} A_{tp} \langle l' m_l' | C_{tp} | l m_{lk} \rangle (\langle r^t \rangle \delta(l',l) - r^t) \frac{1}{r} P_{nl}. \quad (14)$$

Equating Eqs. (12) and (14) and writing

$$u_{cf}(nlm_{lk} \rightarrow l' m_l') = 2 \sum_{tp} A_{tp} \langle l' m_l' | C_{tp} | l m_{lk} \rangle \times w^t_{cf}(nl \rightarrow l'),$$

we obtain the pure radial differential equations

$$\left[-\frac{d^2}{dr^2} + \frac{l'(l'+1)}{r^2} + 2[v_{HF}(nl) - \varepsilon_{nl}] \right] w^t_{cf}(nl \rightarrow l') = [\delta(l,l') \langle r^t \rangle_{nl} - r^t] P_{nl}. \quad (15)$$

Here $v_{HF}(nl)$ is the converged effective potential from the Hartree-Fock calculation. Note that, in general, the functions u_{cf} are complex valued. Note also that the troublesome summation over excited states that occurs in the standard Judd-Ofelt theory is completely avoided. Radial differential equations of this kind are easily solved exactly using, e.g., the finite-difference method. To be consistent with Eq. (4) the radial functions w^t_{cf} are orthogonalized using the following Gram-Schmidt expression:

$$w^t_{\perp cf}(nl \rightarrow l') = w^t_{cf}(nl \rightarrow l') - \sum_{n'}^{occ} P_{n'l'} \times \int w^t_{cf}(nl \rightarrow l') P_{n'l'} dr. \quad (16)$$

For the first matrix element of Eq. (8) we obtain

$$\langle \phi^1_{m,cf} | d^1_q | \phi^0_n \rangle = 2 \delta(m_{sm}, m_{sn}) \sum_{l' m_l' tp} A^*_{tp} \times \int w^t_{\perp cf}(nl \rightarrow l') r P_{nl} dr \times \langle l' m_l' | C_{1q} | l m_{ln} \rangle \langle l' m_l' | C_{tp} | l m_{lm} \rangle.$$

The spherical harmonical matrix elements are then expressed in terms of $3j$ symbols and the procedure is repeated for the second term in Eq. (8) giving

$$d_{cf\text{-}0} = 2 \delta(m_{sm}, m_{sn}) \sum_{l' t} [l', l] A_{tp} \begin{pmatrix} l' & t & l \\ 0 & 0 & 0 \end{pmatrix} \begin{pmatrix} l' & 1 & l \\ 0 & 0 & 0 \end{pmatrix} \times \int w^t_{\perp cf}(nl \rightarrow l') P_{nl} r dr \times \Bigg[(-1)^p \begin{pmatrix} l' & t & l \\ q+m_{ln} & p & -m_{lm} \end{pmatrix} \begin{pmatrix} l' & 1 & l \\ -q-m_{lm} & q & m_{ln} \end{pmatrix} + (-1)^q \begin{pmatrix} l' & t & l \\ q-m_{lm} & p & m_{ln} \end{pmatrix} \times \begin{pmatrix} l' & 1 & l \\ m_{lm}-q & q & -m_{lm} \end{pmatrix} \Bigg], \quad (17)$$

where $p = m_{lm} - m_{ln} - q$ and $[l_1, l_2, \ldots]$ denotes $(2l_1+1)(2l_2+1)\ldots$. The symmetry of the $3j$ symbols reduces the sum over t to $1 \leqslant t \leqslant l + l'$ for odd t, and l' to $l' = l \pm 1$.

The matrix element of Eq. (9) is evaluated in a similar way as

$$d_{cf\text{-}cf} = 4 \delta(m_{sm}, m_{sn}) (-1)^{q - m_{lm}} \sum_{\tau} [l_m', l_n', l] \times \int w^{t_1}_{\perp cf}(nl \rightarrow l_m') w^{t_2}_{\perp cf}(nl \rightarrow l') r dr \begin{pmatrix} l_m' & 1 & l_n' \\ 0 & 0 & 0 \end{pmatrix} \times \begin{pmatrix} l_m' & t_1 & l \\ 0 & 0 & 0 \end{pmatrix} \begin{pmatrix} l_n' & t_2 & l \\ 0 & 0 & 0 \end{pmatrix} \begin{pmatrix} l_m' & 1 & l_n' \\ -m_{lm}' & q & m_{ln}' \end{pmatrix} \times \begin{pmatrix} l_m' & t_1 & l \\ -m_{lm}' & p_1 & m_{lm} \end{pmatrix} \times \begin{pmatrix} l_n' & t_2 & l \\ -m_{ln}' & p_2 & m_{ln} \end{pmatrix} A_{t_1(-p_1)} A_{t_2 p_2}. \quad (18)$$

The sum over τ stands for a summation over t_1, t_2, p_1, p_2, l_m', and l_n'. From the $3j$ symbols it is apparent that $l_m' = l_n' \pm 1$, $|l - t_1| \leqslant l_m' \leqslant l + t_1$, $|l - t_2| \leqslant l_n' \leqslant l + t_2$ and that $t_1 + t_2$ and $l_m' + l_n'$ are odd integers. There is, however, no upper limit to the values of t_1 and t_2; so the sum must be truncated, see Sec. V. As expected, the lower limit is t_1 and $t_2 = 1$, since Eq. (18) together with the solution of Eq. (15) gives $w^0(nl \rightarrow l) \propto P_{nl}$ and Eq. (16) then gives $w^0_\perp \equiv 0$.

B. Mixed spin-orbit contribution

This contribution to the dipole-transition amplitude is treated in the same way as in the crystal-field case, beginning with the perturbed spin-orbit function

$$\phi^1_{k,so} = \frac{1}{r} \sum_{l' m_l' m_s'} u_{so}(nlm_{lk} m_{sk} \rightarrow m_l' m_s') Y_{l' m_l'} \chi_{m_s'}$$

for which Eq. (11) with the spin-orbit perturbing operator then results in

$$\left[-\frac{d^2}{dr^2}+\frac{l'(l'+1)}{r^2}+2[v_{HF}(nl)-\varepsilon_{nl}]\right]w_{so}(nl\rightarrow l)$$
$$=[\langle\xi\rangle_{nl}-\xi_{nl}(r)]P_{nl} \quad (19)$$

with $u_{so}=2\langle lsm_l'm_s'|\hat{l}\cdot\hat{s}|lsm_{lk}m_{sk}\rangle w_{so}$. After the insertion of ϕ_{so}^1 and ϕ_{cf}^1 into the matrix elements of Eq. (10) we obtain

$$\langle\phi_{m,so}^1|d_q^1|\phi_{n,cf}^1\rangle=4\sum_{l'tp}(-1)^q[l',l]A_{tp}\begin{pmatrix}l' & t & l\\ 0 & 0 & 0\end{pmatrix}\times\begin{pmatrix}l' & 1 & l\\ 0 & 0 & 0\end{pmatrix}\begin{pmatrix}l' & t & l\\ -m_{ln}' & p & m_{ln}\end{pmatrix}\times\begin{pmatrix}l' & 1 & l\\ -m_{lm}' & q & m_{ln}'\end{pmatrix}\times\langle lsm_{lm}'m_{sn}|\hat{l}\cdot\hat{s}|lsm_{lm}m_{sm}\rangle\times\int w_{\perp so}w_{\perp cf}^t r\,dr \quad (20a)$$

and

$$\langle\phi_{m,cf}^1|d_q^1|\phi_{n,so}^1\rangle=4\sum_{l'tp}(-1)^p[l',l]A_{t-p}\begin{pmatrix}l' & t & l\\ 0 & 0 & 0\end{pmatrix}\times\begin{pmatrix}l' & 1 & l\\ 0 & 0 & 0\end{pmatrix}\begin{pmatrix}l' & t & l\\ -m_{lm}' & p & m_{lm}\end{pmatrix}\times\begin{pmatrix}l' & 1 & l\\ -m_{lm}' & q & m_{ln}'\end{pmatrix}\times\langle lsm_{ln}'m_{sm}|\hat{l}\cdot\hat{s}|lsm_{ln}m_{sn}\rangle\times\int w_{\perp so}w_{\perp cf}^t r\,dr, \quad (20b)$$

respectively. Note that w_{so} is made orthogonal in the same way as in Eq. (16). The summations over l' and t have the same range as in Eq. (17).

IV. CRYSTAL-FIELD CALCULATIONS

In order to be able to calculate intensities we need access to odd crystal-field parameters (and both even and odd for the $d_{cf\text{-}cf}$ computation). The odd parameters are, however, not generally accessible from experimental fittings. We are interested here in the tetragonal (space group: $I4_1/a$) $LiYF_4$ crystal.[32] The applied coordinate system is defined as follows: x and z axes are along the crystal a and c axes, respectively, with the origin in a rare-earth site. The simplest way to get a reasonable estimate of the crystal-field parameters is to apply the self-consistent electrostatic model, see, e.g., Ref. 23. We believe that this model is appropriate for *ionic* crystals.

In this approach we calculate both the odd and even A_{tp}'s according to

TABLE II. Crystal dipole, quadrupole, and octopole polarizabilities.

Ion	$\alpha^{(dip)}$(Å^3)	$\alpha^{(quad)}$(Å^5)	$\alpha^{(oct)}$(Å^7)
Li^+	0.0344	0.0047	0.0026
Y^{3+}	0.87	1.061	0.58
F^-	0.731	0.631	0.4

$$A_{tp}=(-1)^{p+1}\int\frac{\rho(\vec{R})}{R^{t+1}}C_{t-p}(\theta,\varphi)d\vec{R}$$

with $\rho(\vec{R})$ being the external charge density and $C_{t-p}(\theta,\varphi)$ is a spherical tensor of rank t and projection $-p$. The density $\rho(\vec{R})$ is assumed not to overlap severely between the ligands and the rare-earth ion. A_{tp} can then be expanded using standard monopole, dipole, quadrupole and octopole moments. The crystal-field parameters may thus be written as

$$A_{tp}\approx(-1)^{p+1}\sum_j\left[q_jR_j^{-t-1}+\mu_jR_j^{-t-2}(t+1)+\frac{1}{4}Q_jR_j^{-t-3}(t+2)(t+1)+\frac{1}{12}O_jR_j^{-t-4}(t+3)(t+2)(t+1)\right]C_{t-p}(\theta_j,\varphi_j),$$

where $\mu_j=\alpha_j^{(dip)}E_j$, $Q_j=\alpha_j^{(quad)}dE_j/dR_j$ and $O_j=\alpha_j^{(oct)}d^2E_j/d^2R_j$. E_j, dE_j/dR_j, and d^2E_j/d^2R_j are simply the projections of the total electric field and gradients in the $\vec{R}_j$ direction at site j ($\vec{R}_j$ is the vector from the rare-earth site to the ligand site j). In order to get converged electric fields E_j they need to be calculated self-consistently, i.e., electrostatic equilibrium of charges and induced dipoles at each ion site is ensured. Usually the self-consistent method involves a matrix equation but here we instead find it convenient to solve it iteratively. First the initial electric fields for the ions are calculated using formal point charges. These fields are then submitted into the charged dipole potential expression: $V_j=\Sigma_{i\neq j}q_i/r_i+\alpha_i\vec{E}_i\cdot\vec{r}_i/r_i^3$ and the improved electric fields are obtained through the identity $\vec{E}_j=-\mathrm{grad}V_j$. All these improved fields are then submitted back into the potential expression. The iteration process continues until convergence is fulfilled. All summations are performed for a spherical cluster with radius 100 Å (rare-earth ion at the origin). The self-consistent treatment is carried out only for ion sites within 12 Å from the rare-earth ion. Outside this 12-Å sphere, the electric fields are due to point charges only. This approximation greatly speeds up the process, and several convergence tests also indicate that nearly the same result for A_{tp} is obtained as if all ions were treated self-consistently. Finally, the converged field E_j (in the $\vec{R}_j$ direction) and the derivatives dE_j/dR_j and d^2E_j/d^2R_j are also computed. Table II shows the estimated crystal ion polarizabilities, see Refs. 12, 33, and 34. For the octopole estimations, see Ref. 35.

TABLE III. Crystal-field parameters A_{tp} in atomic units for YLF. Crystallographic data from Ref. 32.

tp	Re A_{tp}	Im A_{tp}
10	2.00×10^{-2}	
11	-4.17×10^{-3}	-2.63×10^{-3}
20	3.44×10^{-3}	
32	-2.04×10^{-3}	1.05×10^{-4}
40	-1.83×10^{-3}	
44	2.90×10^{-3}	
52	1.40×10^{-3}	3.79×10^{-5}
60	4.85×10^{-6}	
64	2.39×10^{-4}	3.08×10^{-5}
72	-3.20×10^{-6}	1.90×10^{-6}
76	-6.51×10^{-5}	8.67×10^{-6}

As is well known, the site symmetry of the substituted rare-earth ion in the present test crystal $LiYF_4$ is S_4. As a result, the potential $V=\Sigma_{tp}A_{tp}r^tC_{tp}$ is invariant with respect to the symmetry operations of the group S_4, consisting of the elements E, IC_4^{-1}, C_2, and IC_4, implying that $A_{1p}\equiv0$. However, the spectra studied in the present work are taken at room temperature and the ions will vibrate. The dynamical environment causes the S_4 symmetry to be slightly broken. The ions break the symmetry instantaneously and thus $A_{1p}\neq0$. This results in an *increased* contribution to the intensity (in, e.g., Judd-Ofelt theory, intensities depend on terms of the type $|A_{tp}|^2$; this can essentially also be observed in the present intensity theory). It is then realized that an intensity average over the various environments results in an effective nonzero value for A_{1p}. We do not include the dynamical effect for higher-order odd parameters because their dynamical variations are much smaller. For an introduction to the connection between molecular dynamics (MD) and optical properties of rare-earth ions, see, e.g., Refs. 36–40. In particular, for $LiYF_4$, A_{1p} and $|A_{1p}|^2$ were calculated earlier using MD and then averaged using several thousands of environments.[12] Instead of zero, the A_{1p}'s were found to vary in the order of $\pm10^{-2}$ a.u. Calculated *ab initio* B_{tp}'s (or A_{tp}'s) are usually rotated in order to make $\mathrm{Im}\,B_{44}=0$, see, e.g., Ref. 23 or 41. This is an approximate way to make it possible to compare calculated parameters with fitted parameters in the reduced S_4-symmetry approach (R approach where $\mathrm{Im}\,B_{44}=0$).[42] It is also beneficial here to attempt to maintain the same coordinate system for both the energy and polarized-intensity calculations since otherwise it would be inconsistent to use the energy eigenvectors in the transition formulas. Table III shows our computed A_{tp}'s rotated to make $\mathrm{Im}\,A_{44}=0$ (using $e^{-im\varphi}A_{tp}$ with $\varphi=33.76°$). For $LiYF_4$ the so-called "$\mathrm{Im}\,B_4^6/\mathrm{Re}\,B_4^6$ ratio" is 0.132 (see p. 2057 in Ref. 43), in good agreement with our $\mathrm{Im}\,A_{64}/\mathrm{Re}\,A_{64}$ ratio.

TABLE IV. Radial integrals in a.u. for Nd^{3+}.

	t			
	1	3	5	7
$S^t(d)$	-7.11×10^{-1}	-3.35	-2.25×10^{1}	
$S^t(g)$	-2.02×10^{-1}	-8.00×10^{-1}	-5.71	-6.37×10^{1}
$R^t(d)$	-1.82×10^{-3}	-9.35×10^{-3}	-7.04×10^{-2}	
$R^t(g)$	-3.97×10^{-4}	-2.37×10^{-3}	-2.22×10^{-2}	-3.04×10^{-1}

TABLE V. Radial integrals in a.u. for Ho^{3+}.

	t			
	1	3	5	7
$S^t(d)$	-2.99×10^{-1}	-1.08	-5.73	
$S^t(g)$	-9.42×10^{-2}	-2.80×10^{-1}	-1.57	-1.41×10^{1}
$R^t(d)$	-1.33×10^{-3}	-5.35×10^{-3}	-3.24×10^{-2}	
$R^t(g)$	-3.19×10^{-4}	-1.48×10^{-3}	-1.11×10^{-2}	-1.23×10^{-1}

V. SIMULATION OF ABSORPTION SPECTRA

Energy levels of the nf^N states and the coefficients c_a^i of Eq. (3) are obtained by diagonalizing the full matrix $\hat{H}'_{eff}$ in Eq. (1). All operators interact simultaneously thus allowing a complete mixing of quantum numbers. The differential equations (15) and (19) are solved by applying the finite-difference method. This results in a matrix equation $A\vec{x}=\vec{b}$, which is solved using the DGTSV routine in the linear algebra program library LAPACK.[44] Using the grid $0<r<20$ a.u. with step length 10^{-4} a.u., the converged perturbed functions are computed and then orthogonalized. Numerical values of the radial integrals in Eqs. (17), (20a), and (20b)

$$S^t(l')=\int w^t_{\perp cf}(nl\rightarrow l')P_{nl}rdr,$$

$$R^t(l')=\int w_{\perp so}(nl\rightarrow l)w^t_{\perp cf}(nl\rightarrow l')rdr$$

are displayed in Tables IV, V, VI, and VII for Nd^{3+}, Ho^{3+}, Er^{3+}, and Tm^{3+}, respectively. When evaluating the contributions from $d_{cf\text{-}cf}$, the summation was truncated at t_1 and $t_2=7$. The radial integrals of Eq. (18) are too many to be tabulated here since already a truncation at t_1 and $t_2=7$ gives 63 contributing integrals involving 25 perturbed functions.

Smentek has earlier reported numerical values of integrals denoted $R_1^t(l')$.[3] These are equal to our $R^t(l')$ multiplied with 4 [$R_1^t(l')=4R^t(l')$]. Note that Smentek's perturbed functions are obtained by replacing $\langle\xi\rangle_{nl}-\xi_{nl}(r)$ with $\langle r^{-3}\rangle_{nl}-r^{-3}$ in Eq. (19). This type of spin-orbit function is

TABLE VI. Radial integrals in a.u. for Er^{3+}.

	t			
	1	3	5	7
$S^t(d)$	-2.75×10^{-1}	-9.66×10^{-1}	-5.00	
$S^t(g)$	-8.65×10^{-2}	-2.50×10^{-1}	-1.37	-1.21×10^{1}
$R^t(d)$	-1.32×10^{-3}	-5.15×10^{-3}	-3.05×10^{-2}	
$R^t(g)$	-3.16×10^{-4}	-1.42×10^{-3}	-1.05×10^{-2}	-1.14×10^{-1}

TABLE VII. Radial integrals in a.u. for Tm^{3+}.

	t			
	1	3	5	7
$S^t(d)$	-2.55×10^{-1}	-8.71×10^{-1}	-4.40	
$S^t(g)$	-7.98×10^{-2}	-2.25×10^{-1}	-1.21	-1.05×10^{1}
$R^t(d)$	-1.31×10^{-3}	-4.99×10^{-3}	-2.89×10^{-2}	
$R^t(g)$	-3.13×10^{-4}	-1.38×10^{-3}	-9.98×10^{-3}	-1.07×10^{-1}

strictly valid for an electron in a pure Coulomb potential only. We have recalculated these integrals (with $\xi=r^{-3}$) for Pr^{3+}, Eu^{3+}, Gd^{3+}, and Tm^{3+} using both classic and relativistic wave functions. The resulting values are shown in Table VIII, note that numerical values are also given for $t=7$ (g perturbations). From this comparison it is clear that Smentek used classical wave functions. It is also known that the relativistic Hartree-Fock solutions of Cowan are very good. For example, they, in general, agree well with more advanced codes such as the MCDF code by Parpia, Froese Fischer, and Grant.[45] All results below are based on relativistic wave functions of Cowan.

The oscillator strengths P_q of Eq. (2) are calculated for every pair of states within the desired region of transition wavelength. The spectra are simulated by plotting

$$P_q\overline{\lambda}^2 \propto \int \alpha(\lambda)d\lambda,$$

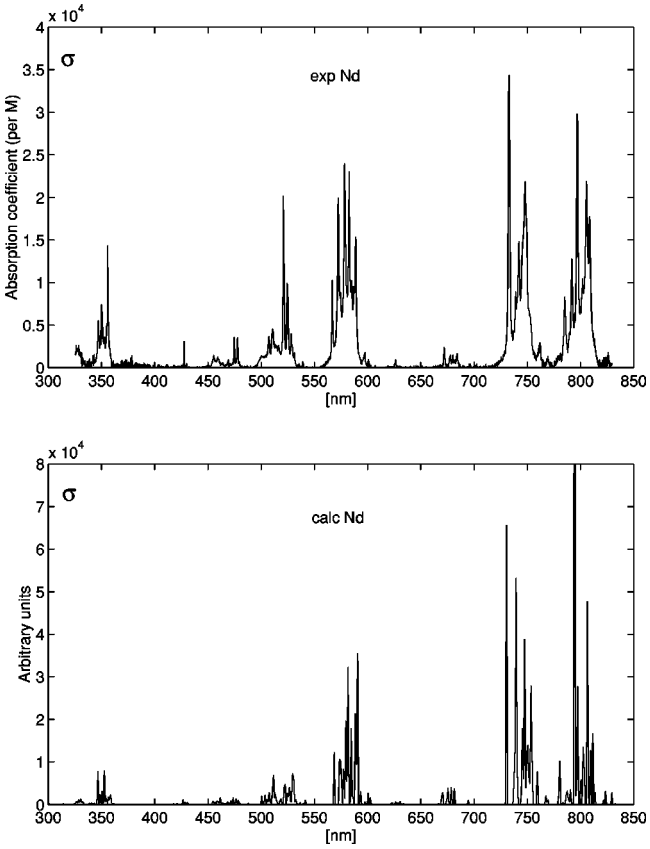

FIG. 1. σ-polarized absorption spectra for Nd^{3+}:YLF (resolution, 1 nm).

TABLE VIII. Our calculated $4R^t(l')$ compared with $R_1^t(l')$ of Ref. 3 in a.u.

	t	Pr^{3+}	Eu^{3+}	Gd^{3+}	Tm^{3+}
$R_1^t(d)$	1	-5.2509	-2.4887	-2.1742	-1.2931
	3	-25.3936	-10.3939	-8.7956	-4.5549
	5	-175.6036	-62.8266	-51.6931	-23.8172
$4R^t(d)$ (classical)	1	-5.5402	-3.8149	-3.5774	-2.8528
	3	-27.2774	-15.8503	-14.3368	-9.7880
	5	-192.3241	-95.3022	-83.4464	-49.8327
$4R^t(d)$ (relativistic)	1	-9.1140	-5.9925	-5.6099	-4.5570
	3	-49.2784	-27.3978	-24.7766	-17.4298
	5	-389.9145	-185.4227	-162.6420	-101.5429
$R_1^t(g)$	1	-1.1839	-0.7553	-0.6911	-0.4817
	3	-6.5310	-3.4375	-3.0268	-1.8027
	5	-56.4390	-24.9862	-21.2651	-11.0496
$4R^t(g)$ (classical)	1	-1.3732	-1.0185	-0.9628	-0.7754
	3	-7.5513	-4.6582	-4.2453	-2.9489
	5	-64.9600	-33.9299	-29.9309	-18.2667
	7	-810.8867	-362.7453	-310.4961	-168.2787
$4R^t(g)$ (relativistic)	1	-1.9118	-1.3973	-1.3228	-1.0898
	3	-12.1551	-7.3718	-6.7369	-4.8524
	5	-120.8008	-61.9738	-54.9103	-35.2550
	7	-1736.079	-762.6581	-656.8033	-379.9514

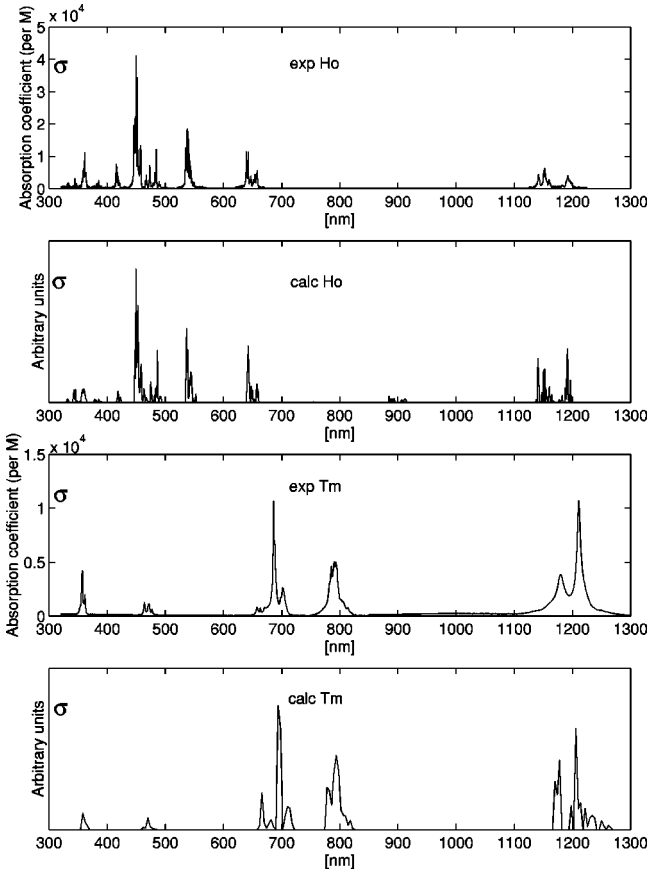

FIG. 2. σ-polarized absorption spectra for Ho^{3+} and Tm^{3+}:YLF (resolutions, 1 nm and 4 nm, respectively).

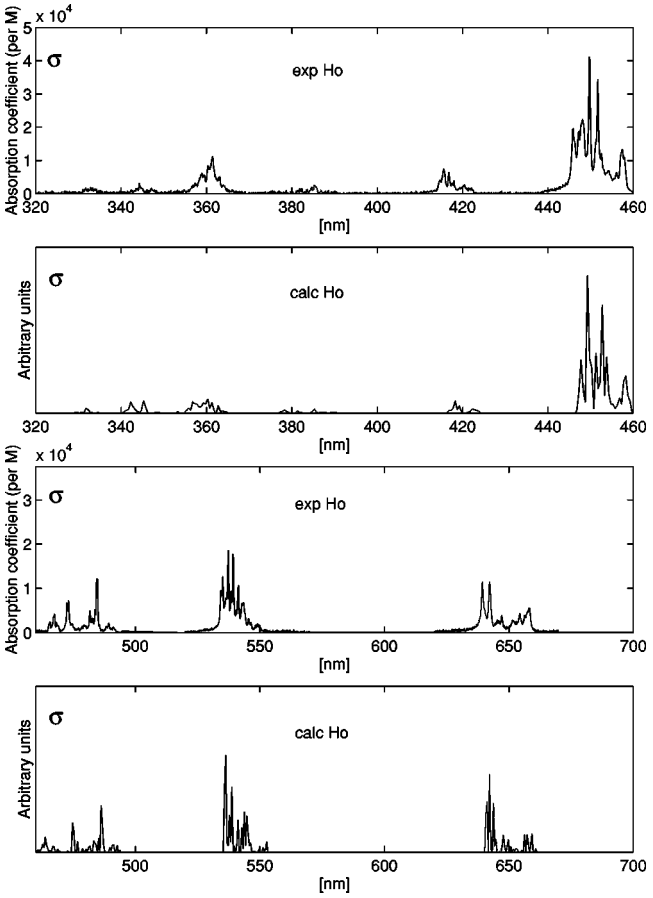

FIG. 3. σ-polarized absorption spectra for Ho^{3+}:YLF (resolution, 0.5 nm).

where α is the absorption coefficient, see Ref. 46. To simulate the resolution of the experimental spectra, P_q has been summed in appropriate intervals for which $\overline{\lambda}$ is the average wavelength.

A comparison of theoretical and experimental σ-polarized absorption spectra for Nd:YLF is shown in Fig. 1. For Ho^{3+} and Tm^{3+}, the σ-polarized spectra are displayed in Fig. 2. Figure 3 shows the fine structure of Ho:YLF. The experimental data are available from LSB's Database Lasers.[47] The last figure shows the theoretical result in the case of Er:YLF. An experimental spectrum is available in Ref. 48. The overall behavior of all spectra agrees well with experiment. The Nd spectrum exhibits the largest discrepancy; although the main features are reproduced, we observe deviations in some of the bands, particularly for wavelengths at 350 and 450–550 nm. Among several possibilities, this could be an indication that correlation effects are more important for Nd. Correlation should be more pronounced for loosely bound electrons such as for ions at the beginning of the RE series, compared to the end of the series. As an example we have calculated the correlation contributions for polarizabilities as in Ref. 34 (they have the same type of transition elements). For Nd^{3+}, $\alpha_1 = -0.203$ Å^3 while for Ho^{3+}, $\alpha_1 = -0.0649$ Å^3. As expected, the influence of correlation is much larger for Nd^{3+} than for Ho^{3+}.

The Tm spectrum in Fig. 2 is in quite good agreement with the experimental bands, except for the transition around 360 nm, which should be slightly more prominent. For Ho, the simulated spectrum is very successful as can be seen in Fig. 2. The overall band shapes are in excellent agreement with the experimental results. The $^5I_8 \rightarrow {}^5J_6$ transitions in the 1100–1200 nm region are, however, slightly more pro-

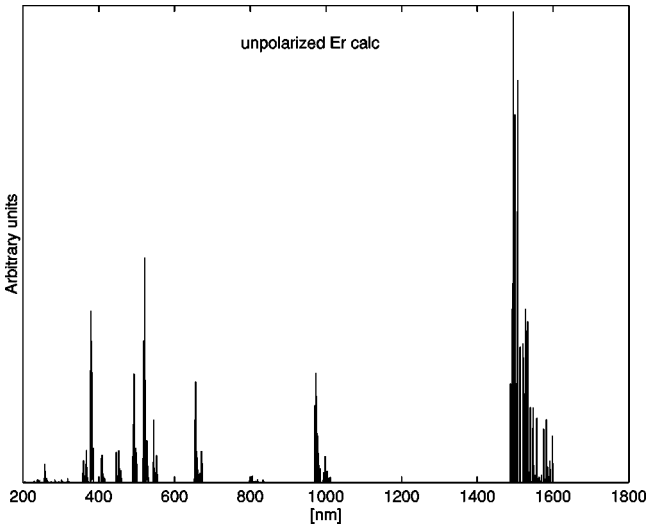

FIG. 4. Unpolarized absorption spectrum for Er^{3+}:YLF (resolution, 0.5 nm).

TABLE IX. Relative σ-polarized oscillator strengths from $d_{cf\text{-}0}$, $d_{so\text{-}cf}$, and $d_{cf\text{-}cf}$.

	$P_{cf\text{-}0}$	$P_{so\text{-}cf}$	$P_{cf\text{-}cf}$
Nd	1.0	9.9×10^{-5}	8.4×10^{-3}
Ho	1.0	4.6×10^{-4}	1.9×10^{-3}
Er	1.0	3.4×10^{-4}	1.7×10^{-3}
Tm	1.0	2.5×10^{-4}	1.6×10^{-3}

nounced than the experimental measurements. The fine structure in Fig. 3 also agrees well with experiment. It is questionable if the transitions between the Stark states ever can be reproduced exactly, even with fitted intensity parameters. Besides the theoretical difficulties, the variation of experimental techniques and samples also leads to sensitivities in the spectra at the fine-structure level.

Erbium is an extremely important ion in todays fiber technology, we have therefore also calculated the spectrum in this case, see Fig. 4, and for a comparison to experiment see Ref. 48. It is very interesting to see that nearly all bands are reproduced. Even at the fine-structure level the results are convincing, although not exact. Actually, the only real deviation is the peak slightly above 200 nm, where our peak is too weak.

It has been speculated that the contributions from $d_{so\text{-}cf}$ and possibly $d_{cf\text{-}cf}$ could be important for transition intensities.[3–5] In order to compare the magnitudes of their influences we have calculated oscillator strengths using the elements $d_{cf\text{-}0}$, $d_{so\text{-}cf}$, and $d_{cf\text{-}cf}$ separately. Note, however, that it is clear from Eqs. (2) and (7) that such a superpositional division is only approximate. The sum of all oscillator strengths are then normalized such that the $d_{cf\text{-}0}$ part equals unity. The summation was made using σ polarization for all transitions from the ground states to the other excited f states. The results are given in Table IX. Thus contrary to earlier beliefs, the impact of these third-order effects is actually quite small, at least for ground-state excitations in the RE:YLF crystal.

VI. CONCLUSION

An alternative and improved intensity theory has been formulated. Good agreement between calculations and experiment is demonstrated. Higher-order amplitudes ($d_{so\text{-}cf}$ and $d_{cf\text{-}cf}$) seem to be almost negligible in $LiYF_4$. Although this could be interpreted as that the Judd-Ofelt theory is reasonably sound, it should be remembered that our approach has also removed the intrinsic approximations in that model. The present intensity model based on perturbed functions is therefore preferable in order to obtain as accurate results as possible. Certain forbidden or weak transitions at the ''Judd-Ofelt level'' also motivate the use of higher-order amplitudes. It is also possible that they could be more pronounced in materials having very different crystal-field parameters than those in YLF. It is still unclear how important the contributions from correlation effects actually are. A quantitative investigation is in progress.

ACKNOWLEDGMENTS

Grants from Mid Sweden University, ACREO Fiber Laboratory (Hudiksvall), Teknikbrostiftelsen (Umeå), and KK-stiftelsen are greatly acknowledged. Fruitful discussions with Lidia Smentek are appreciated. Support from B. Johansson and O. Eriksson (Uppsala University) is also appreciated.

[1] B. R. Judd, Phys. Rev. **127**, 750 (1962).
[2] R. M. Sternheimer, M. Blume, and R. F. Peierls, Phys. Rev. **173**, 376 (1968).
[3] L. Smentek, J. Phys. B **32**, 593 (1999).
[4] G. W. Burdick, M. C. Downer, and D. K. Sardar, J. Chem. Phys. **91**, 1511 (1989).
[5] M. F. Reid, J. Alloys Compd. **193**, 160 (1993).
[6] K. Jankowski, L. Smentek-Mielczarek, and A. Sokolowski, Mol. Phys. **59**, 1165 (1986).
[7] L. Smentek and B. Andes Hess, J. Chem. Phys. **89**, 703 (1988).
[8] H. P. Kelly, Adv. Chem. Phys. **14**, 129 (1969).
[9] G. S. Ofelt, J. Chem. Phys. **37**, 511 (1962).
[10] S. Edvardsson, M. Klintenberg, and J. Thomas, Phys. Rev. B **54**, 17 476 (1996).
[11] S. Edvardsson and D. Åberg, Comput. Phys. Commun. **133**, 396 (2001).
[12] S. Edvardsson and M. Klintenberg, Mater. Sci. Forum **315**, 407 (1999).
[13] S. Edvardsson and M. Klintenberg, J. Alloys Compd. **275**, 230 (1998).
[14] C. Xueyuan and L. Zundu, J. Phys.: Condens. Matter **8**, 2571 (1996).
[15] M. A. Cuoto dos Santos, P. Porcher, J. C. Krupa, and J. Y. Gesland, J. Phys.: Condens. Matter **8**, 4643 (1996).
[16] G. K. Liu, W. T. Carnall, R. P. Jones, R. L. Cone, and J. Huang, J. Alloys Compd. **207**, 69 (1994).
[17] C. Görller-Walrand, K. Binnemans, and L. Fluyt, J. Phys.: Condens. Matter **5**, 8359 (1993).
[18] O. L. Malta, S. J. L. Ribeiro, M. Faucher, and P. Porcher, J. Phys. Chem. Solids **52**, 587 (1991).
[19] C. Görller-Walrand, L. Fluyt, P. Porcher, A. A. S. da Gama, G. F. de S, W. T. Carnall, and G. L. Goodman, J. Less-Common Met. **148**, 339 (1989).
[20] A. A. S. da Gama, G. F. de S, P. Porcher, and P. Caro, J. Chem. Phys. **75**, 2583 (1981).
[21] L. Esterowitz, F. J. Bartoli, R. E. Allen, D. E. Wortman, C. A. Morrison, and R. P. Leavitt, Phys. Rev. B **19**, 6442 (1979).
[22] H. P. Jenssen, A. Linz, R. P. Leavitt, C. A. Morrison, and D. E. Wortmann, Phys. Rev. B **11**, 92 (1975).
[23] M. Faucher and D. Garcia, Phys. Rev. B **26**, 5451 (1982).
[24] M. Klintenberg, S. Edvardsson, and J. O. Thomas, Phys. Rev. B **55**, 10 369 (1997).
[25] C. Duan, S. Xia, W. Zhang, M. Yin, and J. C. Krupa, J. Alloys Compd. **275**, 450 (1998).

[26] Program available at http://gluon.fi.uib.no/AMOS/COWAN/rcn.html
[27] K. Rajnak and B. G. Wybourne, Phys. Rev. **132**, 280 (1963).
[28] B. R. Judd, Phys. Rev. **141**, 4 (1966).
[29] M. Faucher, D. Garcia, and O. K. Moune, J. Alloys Compd. **193**, 210 (1993).
[30] W. T. Carnall, G. L. Goodman, K. Rajnak, and R. S. Rana, J. Chem. Phys. **90**, 3443 (1989).
[31] G. Racah, Phys. Rev. **76**, 1352 (1949).
[32] E. Garcia and R. R. Ryan, Acta Crystallogr., Sect. C: Cryst. Struct. Commun. **C49**, 2053 (1993).
[33] P. C. Schmidt, A. Weiss, and T. P. Das, Phys. Rev. B **19**, 5525 (1979).
[34] S. Edvardsson and D. Åberg, J. Alloys Compd. **303**, 280 (2000).
[35] G. D. Mahan and K. R. Subbaswamy, *Local Density Theory of Polarizability* (Plenum Press, New York, 1990), p. 86.
[36] M. Klintenberg, S. Edvardsson, and J. O. Thomas, J. Lumin. **72**, 218 (1997).
[37] S. Edvardsson and M. Klintenberg, and J. O. Thomas, Phys. Rev. B **54**, 17 476 (1996).
[38] G. Cormier, J. A. Capobianco, C. A. Morrison, and A. Monteil, Phys. Rev. B **48**, 16 290 (1993).
[39] S. Edvardsson, M. Wolf, and J. O. Thomas, Phys. Rev. B **45**, 10 918 (1992).
[40] S. A. Brawer and M. J. Weber, J. Chem. Phys. **75**, 3522 (1981).
[41] L. Esterowitz, F. J. Bartoli, R. E. Allen, D. E. Wortman, C. A. Morrison, and R. P. Leavitt, Phys. Rev. B **19**, 6442 (1979).
[42] C. Rudowicz, Chem. Phys. **97**, 43 (1985).
[43] J. Mulak, Pol. J. Chem. **67**, 2053 (1993).
[44] See http://www.netlib.org/lapack/
[45] F. A. Parpia, C. Froese Fischer, and I. P. Grant, Comput. Phys. Commun. **94**, 249 (1996).
[46] W. B. Fowler and D. L. Dexter, Phys. Rev. **128**, 2154 (1962).
[47] See http://aesd.larc.nasa.gov/gl/laser/dbmain.htm
[48] M. B. Camargoa, L. Gomesa, and I. M. Ranier, Opt. Mater. **6**, 331 (1996).
[49] D. E. Wortman, N. Karayianis, and C. A. Morrison, Harry Diamond Laboratories Report No. TR-1770 (NTIS#033902), 1976 (unpublished).
[50] N. Karayianis, D. E. Wortman, and H. P. Jenssen, Phys. Chem. Solids **37**, 675 (1976).
[51] C. A. Morrison and R. P. Leavitt, in *Handbook on the Physics and Chemistry of Rare-Earths*, edited by K. A. Gschneidner and L. Eyring (North-Holland, Amsterdam, 1982), p. 627.